

Numerical simulation of size effect in rock

Fakhimi, A.

Department of Mineral Engineering, New Mexico Tech, Socorro, NM 87801, USA & Department of Civil Engineering, Tarbiat Modarres University, Tehran, Iran

Akbarzadeh, Y.

Mining Engineering Department, Colorado School of Mines, Golden, CO 80401, USA

Copyright 2005, ARMA, American Rock Mechanics Association

This paper was prepared for presentation at Golden Rocks 2006, The 41st U.S. Symposium on Rock Mechanics (USRMS): "50 Years of Rock Mechanics - Landmarks and Future Challenges.", held in Golden, Colorado, June 17-21, 2006.

This paper was selected for presentation by a USRMS Program Committee following review of information contained in an abstract submitted earlier by the author(s). Contents of the paper, as presented, have not been reviewed by ARMA/USRMS and are subject to correction by the author(s). The material, as presented, does not necessarily reflect any position of USRMS, ARMA, their officers, or members. Electronic reproduction, distribution, or storage of any part of this paper for commercial purposes without the written consent of ARMA is prohibited. Permission to reproduce in print is restricted to an abstract of not more than 300 words; illustrations may not be copied. The abstract must contain conspicuous acknowledgement of where and by whom the paper was presented.

ABSTRACT: Numerous experimental studies show that there is a decrease in strength of rock material with increasing specimen size. This phenomenon is known as size effect in rock mechanics. In this paper, size effect is studied numerically using a discrete element approach. The numerical model is made of cylinders that interact through normal and shear springs. The cylinders are bonded to each other at contact points. This bond can break if the normal or shear contact force exceeds the bond strength. In this way, crack propagation in the numerical model can be simulated. The program Ca2 was used to perform the numerical simulations. The size effect, with and without initial cracks was investigated. Single crack and multiple randomly oriented cracks were introduced in the model and size effect was studied by changing the specimen size. The numerical initial cracks were intended to mimic the observed initial micro cracks or fissures in rock. Numerical uniaxial tensile, compressive, and bending tests were studied. It was shown that while fracture mechanics can explain size effect in tensile and bending tests, for compression tests the initial crack length must be increased faster than the specimen size to be able to capture size effect.

1. INTRODUCTION

Larger specimens of rock are generally weaker than smaller ones. This phenomenon, called size effect or scale effect in rock mechanics, has been studied by several investigators. Mogi [1] tested rectangular prisms of marble with length to width ratio of 2:1. He found a decrease of 11 percent in the rock strength as the specimen length was increased from 0.04 to 0.2 m. Bieniawski [2] investigated uniaxial strength of cubic specimens of coal ranging in size from 0.02 to 2.0 m. He found that the strength decreased by a factor of 7 with increasing size until the strength approached 4.3 MPa. His assumption was that since coal is not a continuous solid material and contains various discontinuities such as cracks, the strength of coal is a statistical value depending on the number and types of discontinuities present. In smaller specimens, the probability of finding flaws is smaller, thus the strength is higher. Pratt et. al. [3] performed

laboratory and in situ uniaxial tests on unjointed specimens of quartz diorite and granodiorite. The in situ tests were conducted on right triangular prisms ranging in length from 0.3 m to 2.7 m and loaded by a flat jack system. They found that the compressive strength of quartz diorite decreased with increasing specimen size by a factor of 10. Van Vliet and Van Mier [4] conducted some uniaxial tension experiments to study size effect in concrete and sandstone. They conducted three series of uniaxial tension tests under varying humidity conditions on concrete and sandstone and observed size effect on the nominal strength.

In this paper, a discrete element numerical model was used to simulate size effect in rock. The two dimensional numerical model is made of small cylinders that interact through normal and shear springs. To represent fissures in rock, initial cracks were generated in the model. Numerical tensile, compressive, and bending tests were performed to investigate size effect.

2. THEORETICAL BACKGROUND

At least there are two approaches to interpret the phenomenon of size effect, namely statistical size effect and fracture mechanics size effect. According to Bazant and Planas [5], size effect in solid mechanics was initially described by Leonardo Da Vinci in the sixteenth century, who stated that “among cords of equal thickness, the longer is the least strong”. Later on, some other scientists observed and studied size effect but the formal formulation of the problem as viewed as a statistical phenomenon was introduced by Weibull [6]. In his theory, Weibull assumed that: a) the probability of failure of a solid body for a given applied stress, is a function of its volume. b) a solid body is made of small units and the chance of its survival under the applied stress is equal to the multiplication of chances of survival of these units. This last assumption means that survival of different parts of the body has been considered as independent events. Although, this assumption is correct for an ideal brittle material, for a quasi-brittle material like rock, it may not be valid. In rock, a process zone that is made of micro cracks is developed close to a crack tip. This can cease the extension of a crack in one part of the specimen and affect the extension of cracks in other regions of the specimen making the second Weibull assumption invalid.

An alternative point of view is to consider fracture mechanics size effect. Fracture mechanics was introduced by Griffith [7], who defined the notion of surface energy as a material property. He argued that due to presence of flaws or cracks, the strength of larger specimens are lower than those of smaller specimens. For example, he showed that by reducing the cross sectional area of glass fibers, the tensile strength increases drastically due to less chance of presence of flaws in smaller specimens.

The fracture mechanics size effect can be explained by using dimensional analysis. In Fig. 1, a specimen with a crack is shown. When a body contains a crack, a strong stress concentration develops around the crack tip. If the behavior of the material is isotropic and elastic, except in a small fracture zone, this stress concentration has the same distribution close to the crack tip and only its intensity varies by changing the magnitude of applied load. The stress intensity factor for the specimen in Fig. 1 is:

$$K_I = f\left(\frac{p}{b}, a, D\right) \quad (1)$$

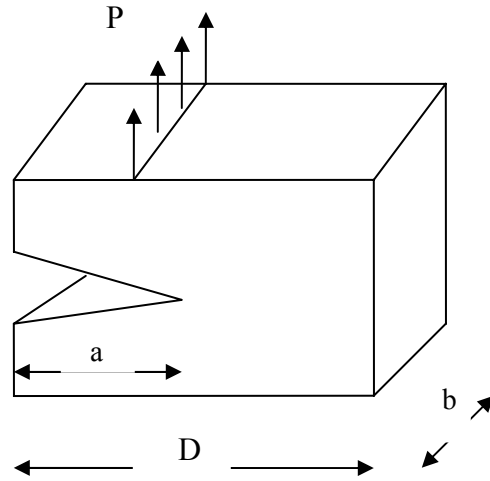


Fig. 1. A specimen with a crack under mode I loading.

where the stress intensity factor was assumed to be a function of applied load per unit thickness, crack length (a), and specimen size (D). Considering the dimensional analysis, the only possible format for dimensionless K_I is as follows:

$$\frac{K_I}{\sqrt{D} \frac{p}{bD}} = g\left(\frac{a}{D}\right) \quad (2)$$

or,

$$K_I = \frac{p}{b\sqrt{D}} g\left(\frac{a}{D}\right) \quad (3)$$

According to the linear fracture mechanics, the crack can extend if the stress intensity factor becomes equal to the fracture toughness (K_{IC}) of the material. Hence, the nominal strength of the body is:

$$\sigma_N = \frac{p}{bD} = \frac{K_{IC}}{\sqrt{D} g\left(\frac{a}{D}\right)} \quad (4)$$

For specimens with proportional dimension, a/D is a constant. Therefore, Eq. 4 demonstrates that by increasing the specimen size (D), the nominal strength of the specimen reduces.

3. THE NUMERICAL MODEL

A discrete element numerical model was used to simulate size effect in rock. In this model, many rigid circular elements (cylinders) that interact through normal and shear springs are used. The normal and shear spring constants are shown as k_n and k_s , respectively. The cylinders are glued at the contact points with the normal and shear bonds (n_b and s_b) to withstand the applied loads. A bond breaks if the force between two cylinders in contact exceeds the normal or shear bond strength. After a bond breakage, a coulomb type frictional law with a friction coefficient of μ governs sliding between adjacent cylinders. Therefore, in the numerical model, the normal and shear spring constants (k_n , k_s), normal and shear bonds (n_b , s_b), friction coefficient (μ), and cylinders radius (R) as micro-parameters must be specified.

CA2 program [8] that is a hybrid explicit finite element-discrete element code was used for numerical analyses. To prepare the numerical model using CA2, first the surrounding flexible walls that consist of a finite element grid, are generated. Then, the cylinders are created that are randomly located within the confined domain between the walls. To reach to equilibrium, the equations of motion are solved together with a contact bond constitutive model with zero normal and shear bonds. The friction coefficient is also zero to let easily movement of the cylinders to fill all the gaps between the surrounding walls. After equilibrium, the induced stress in the surrounding walls is recorded. This is called genesis pressure (σ_0) that is responsible for small overlap of the cylinders. Therefore, a slightly overlapping circular particle interaction (SOCPI) model is developed that compared to a similar model with no particle overlap is more accurate in simulating rock tensile strength and friction angle [9]. Next, locked-in forces between the cylinders are initialized to zero and the cylinders in contact are glued to each other by introducing normal and shear bonds to complete the numerical sample preparation. This sample is now ready to be numerically tested.

An important problem in preparation of the numerical model is the calibration of the model, i.e. to find micro-parameters k_n , k_s , n_b , s_b , μ , R and σ_0 to result in macroscopic properties of a rock such as modulus of elasticity, Poisson's ratio, and uniaxial

strength. The calibration was performed using the technique introduced by Fakhimi and Villegas [10].

4. NUMERICAL MODELING OF SIZE EFFECT

The numerical model was calibrated to result in macroscopic properties similar to Pennsylvania Blue Sandstone. This sandstone has a modulus of elasticity of 27 GPa, Poisson's ratio of 0.15, uniaxial strength of 122 MPa, and Brazilian tensile strength of 9.9 MPa. The calibration was conducted by using the dimensionless charts introduced by Fakhimi and Villegas [10]. Through this calibration procedure, the microscopic parameters of $\sigma_0 = 3.4$ GPa, $k_n = 42.4$ GPa, $k_s = 17.8$ GPa, $n_b = 12664$ N/m, $s_b = 63320$ N/m, $\mu = 0.5$, and $R = 0.5$ mm were obtained. This numerical specimen was used to study size effect in tension, compression, and bending tests.

4.1. Tensile tests

Four numerical uniaxial tests were conducted on specimens without cracks. Specimens with a single crack were tested in direct tensile tests as well. The cracked specimen had a central crack in the middle. The crack length was equal to half of the specimen width. A crack in CA2 is a line between adjacent cylinders in contact that has no normal and shear bond. The normal and shear stiffness of the crack surface was assumed to be the same as that for the cylinders. The numerical specimens tested were 2×4 , 4×8 , 8×16 , and 16×32 cm in dimension. The numerical set up for the direct tensile test of cracked specimen is illustrated in Fig. 2. To conduct the test, the top and bottom of the specimen were glued to the upper and lower numerical platens. The top of upper platen was fixed vertically and the lower one was moved with a constant velocity in the vertical direction. The failed specimen at the end of the test shows that the crack extended in its initial plane as expected (Fig. 3). Fig. 4 shows the tensile strength obtained from these numerical tests as a function of normalized specimen width (D/R), where D is the specimen width and R is the average cylinders radius. This figure shows size effect for both intact and cracked specimens, although the observed size effect for intact specimens may not be extensive enough to simulate size effect for some rocks. The nominal tensile strength for a cracked specimen was defined as the peak load divided by half of the specimen width. If the numerical model is

considered as a fair representation of rock behavior, the results in Fig. 4 demonstrate that extensive size effect in tensile strength of rock is due to presence of initial cracks in rock and the fracture mechanics can explain the size effect in this case.

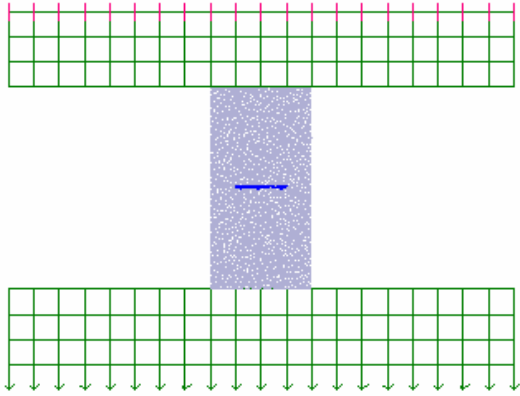


Fig. 2. Numerical uniaxial tensile test set up for a specimen with a crack.

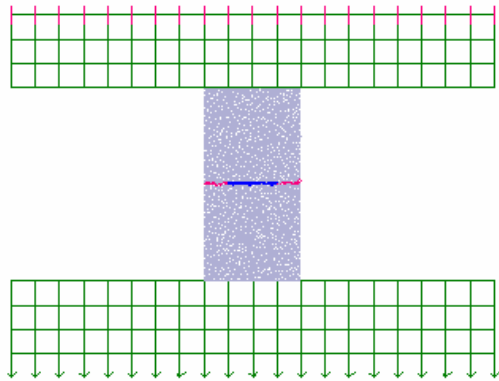


Fig. 3. Numerical specimen in uniaxial tensile test after failure.

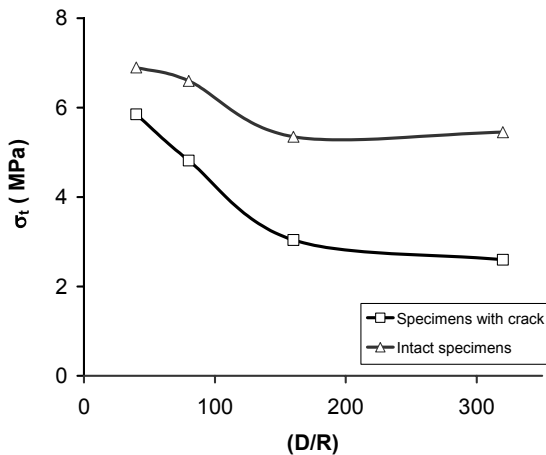


Fig. 4. Tensile strength vs. normalized size for intact specimens and specimens with central cracks.

4.2. Compressive tests

Intact and cracked specimens 1×2 , 2×4 , 4×8 , and 8×16 cm in dimension were tested uniaxially. In the specimens with crack, a crack was generated with a dip angle of 45° to induce a mixed mode failure (Fig. 5). The ratio of the projected length of the crack in the horizontal direction was kept half of the specimen width; crack length was chosen to be in proportion to the specimen size. Two different friction coefficient of $f = 0.0$ and $f = 0.1$ was assumed for the crack surface. The interfaces between the upper and lower platens and the specimen were frictionless. Fig. 6 shows the damaged specimen with the induced cracks. As expected, wing type tensile cracks were developed at the ends of the initial crack. Fig. 7 demonstrates the uniaxial compressive strength of intact specimens and cracked specimens with $f = 0.0$ and $f = 0.1$ versus dimensionless specimen size (D/R). The nominal uniaxial compressive strength of a cracked specimen was defined as the peak load

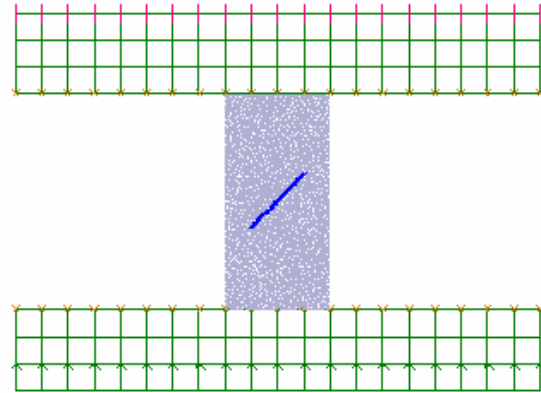


Fig. 5. Numerical compressive test set up for a specimen with a crack.

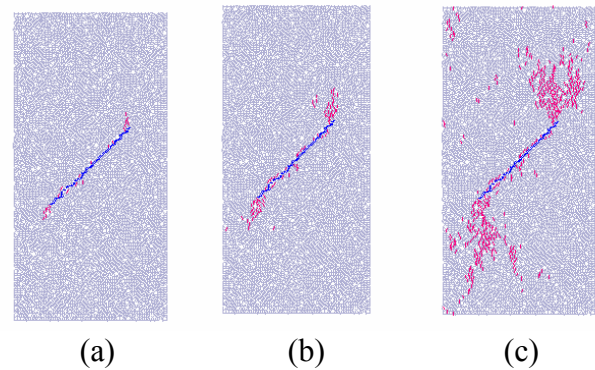


Fig. 6. Crack extension in the uniaxial compressive test as the applied stress from (a) to (c) was increased gradually.

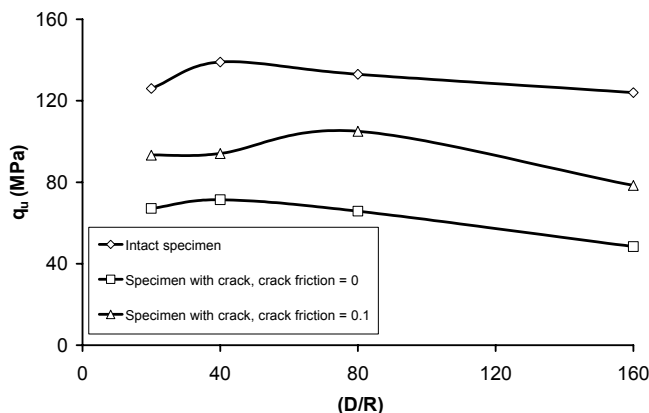


Fig. 7. Uniaxial compressive strength vs. normalized size for intact specimens and specimens with initial cracks.

divided by the total width. As expected, cracked specimens were weaker than the intact ones. In addition, among the cracked specimens, those with lower friction coefficient for the crack surface showed smaller uniaxial strength. An important observation is that no significant size effect could be simulated in the numerical compressive tests. This is true even for specimens with internal cracks. A possible explanation for the absence of extensive size effect in the compressive tests is the distribution of stress close to the crack tips. In fact, even for the compressive tests, small regions of tensile stress exist close to the crack tips, but the size of these tensile regions are smaller than those for the uniaxial tensile tests, leading to less extensive induced size effect.

In an attempt to simulate noticeable size effect in compression tests, initial random cracks were developed in the specimens. These cracks were uniformly distributed in the specimen and their dips were randomly selected in the range of -90° to $+90^\circ$. The idea was to allow the interaction of many cracks, similar to that in a real rock, hoping that a more realistic size effect is observed. Fig. 8 shows the numerical model with the initial randomly oriented and located cracks. The crack density for all specimens was $15000/\text{m}^2$, i.e. 48, 192 and 768 cracks were generated in the specimens 4×8 , 8×16 and 16×32 cm in dimension, respectively. The crack length was 0.002 m for all specimens. Fig. 9 shows the uniaxial strength as a function of specimen size. Although some size effect is observed, it may not be as extensive as that observed for rocks.

From the compression test results, especially those with a single crack, it was concluded that as the specimen size is increased, the initial crack length must be increased at a higher proportion if this numerical model was going to predict realistic size effect. This indicates that fracture mechanics size effect in which the initial crack length is assumed to be proportional to specimen size may not be capable to interpret the size effect in this numerical model. Therefore, the following exponential function was suggested for relationship of average crack length and specimen size in a two dimensional analysis, if extensive size effect is going to be modeled:

$$L = (1.0 - \exp(-\alpha DB))L' \quad (5)$$

where L is the average length of cracks, L' is the crack length for very large specimens, D and B are width and height of the specimen, and α is a constant that depends on the rock type.

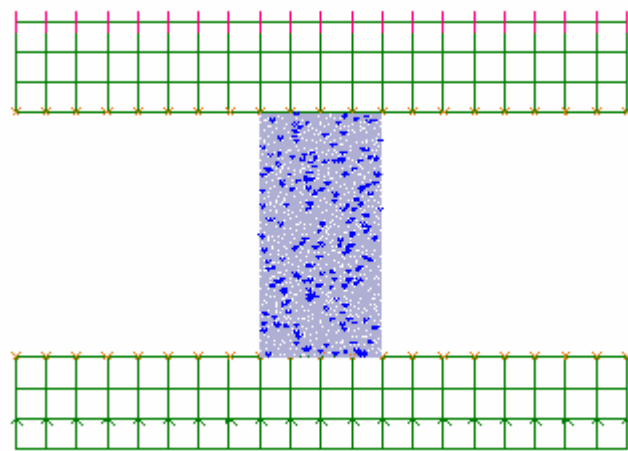


Fig. 8. Numerical compressive test set up for a specimen with randomly oriented and located initial cracks.

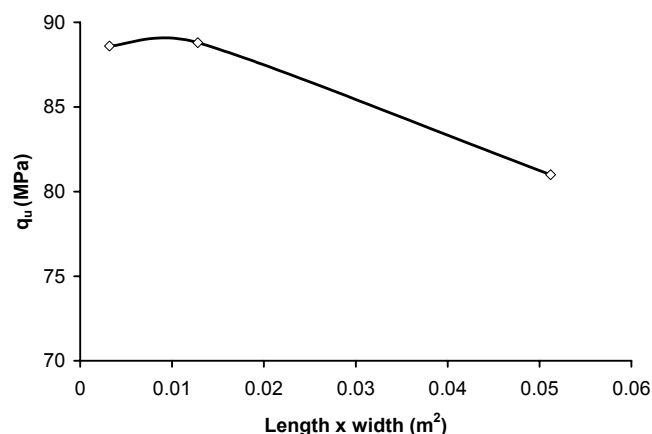


Fig. 9. Uniaxial compressive strength vs. area for specimens with randomly oriented and located initial cracks.

Figs. 10 and 11 show the simulated size effect for compressive and tensile tests. 60000/m² cracks were used in the simulations. Two different α value of 100 and 200 and $L' = 0.01$ m were assumed. These figures show significant simulated size effect. In reality, the α parameter can be modified to result in the size effect similar to that of a rock. Note that the simulated size effect in tension is more intensive compared to that of compression tests. This indicates that the presence of cracks has more drastic effect on tensile strength that should be expected.

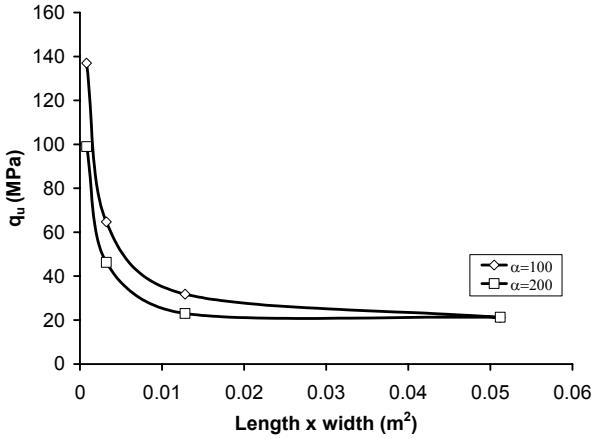


Fig. 10. Uniaxial compressive strength vs. area for specimens with randomly oriented and located initial cracks. The length of initial cracks was assumed to increase faster than the specimen size.

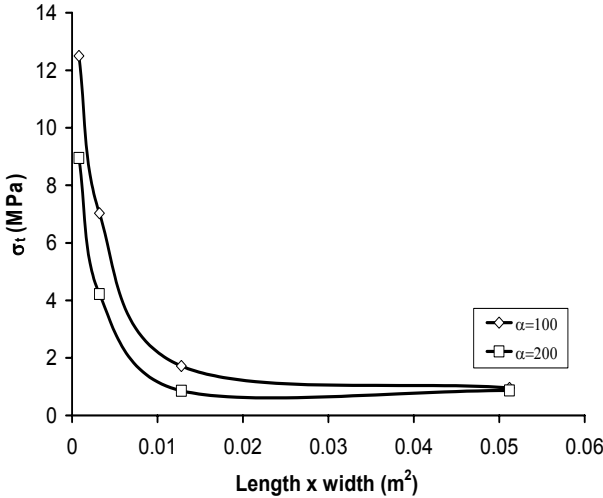


Fig. 11. Uniaxial tensile strength vs. area for specimens with randomly oriented and located initial cracks. The length of initial cracks was assumed to increase faster than the specimen size.

4.3. Bending tests

Three point bending tests were conducted on numerical specimens with micromechanical properties identical to those for uniaxial tests. Numerical results for intact specimens showed no meaningful size effect. Hence, bending specimens with initial notches in the middle of the beams were investigated. For a notched beam, in a three point bending test (Fig. 12), the stress intensity factor is [11]:

$$K_I = \frac{(1.99 - \frac{a}{D}(1 - \frac{a}{D})(2.15 - 3.93\frac{a}{D} + 2.7(\frac{a}{D})^2))}{2(1 + \frac{2a}{D})(1 - \frac{a}{D})^{1.5}} \times \frac{3P}{b\sqrt{D}} \frac{S}{D} \sqrt{\frac{a}{D}} \quad (6)$$

where S is the beam span, D is the beam height, P is the applied load, and a is the notch length. The axial tensile stress in the vicinity of the notch tip is:

$$\sigma = \frac{K_I}{\sqrt{2\pi r}} \quad (7)$$

where r is the distance from the crack tip. In order to extend the crack in the numerical model, the total axial force (F) applied to a cylinder with radius R and unit length, must be equal to the normal bond (n_b), i.e.

$$F = \int_0^{2R} \frac{K_I}{\sqrt{2\pi r}} dr = n_b \quad (8)$$

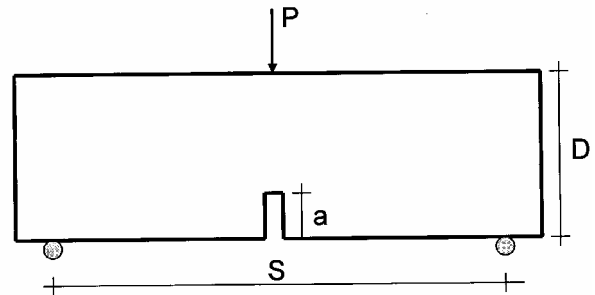


Fig. 12. Three point bending test of a notched beam.

It is interesting to note that Eq. 8 is consistent with nonlocal continuum approach in which a weighted average of stress or strain in a region around a point is used to dictate the crack extension. By combining equations 6, 7 and 8 for a three point beam test, the failure load is obtained:

$$P_{\max} = \frac{bn_b\sqrt{\pi D}\left(1 + \frac{2a}{D}\right)\left(1 - \frac{a}{D}\right)^{1.5}}{3\sqrt{R}\frac{S}{D}\sqrt{\frac{a}{D}}} \times \frac{1}{1.99 - \frac{a}{D}\left(1 - \frac{a}{D}\right)(2.15 - 3.93\frac{a}{D} + 2.7(\frac{a}{D})^2)} \quad (9)$$

where b is the beam width. The beams tested were geometrically similar with constant S/D and a/D values. Hence, the nominal bending strength of the beam, defined as:

$$\sigma_N = \frac{P_{\max}}{bD} \quad (10)$$

is proportional to $1/\sqrt{D}$. This means that the numerical model should capture the fracture mechanics size effect. Beams 1×3 , 2×6 , 4×12 , and 8×24 cm in dimension were used with a central notch for numerical modeling. The notch length was 20% of the beam height in the tests. In Fig. 13, the nominal beams strengths, obtained from numerical tests are compared with those from the closed form solution (Eqs. 9, 10). As Fig. 13 demonstrates, size effect was captured by both numerical and analytical methods, but even though the trends of the two curves are similar, the strengths of numerical specimens are higher than those from closed form solution. This is due to the irregular arrangement of the cylinders; when the crack reaches a cylinder, it must change its path to extend along the contact points. This requires additional energy compared to the theoretical analysis in that the crack path was assumed to be straight.

As mentioned earlier, numerical bending tests on intact specimens did not show noticeable size effect. To improve the simulation of size effect, initial random cracks were developed in the specimen. These cracks, similar to the uniaxial tests, were uniformly distributed in the specimen and their dips were randomly selected in the range of -90° to $+90^\circ$.

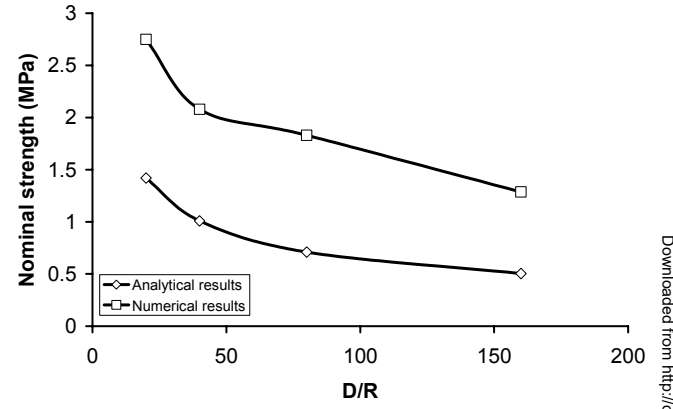


Fig. 13. Analytical and numerical nominal strengths of beam specimens with a center notch tested in three point bending tests vs. normalized size.

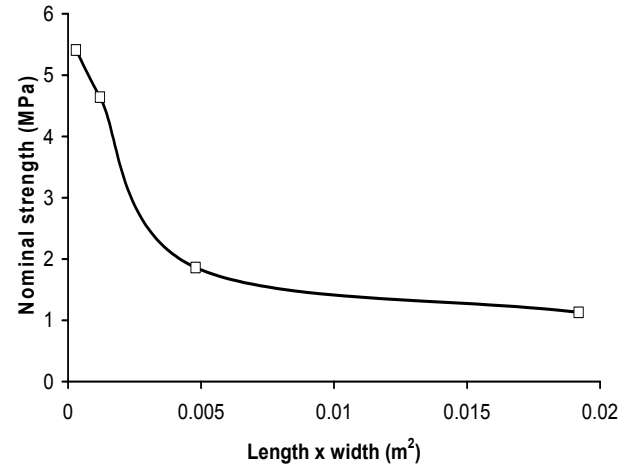


Fig. 14. Numerical nominal strength of beam specimens with randomly oriented and located cracks tested in three point bending test vs. specimen area. The initial crack lengths were increased faster than the specimen size.

The lengths of initial cracks were increased by increasing the specimen size as is dictated by Eq. 5. The crack parameter, α , of 100 and L' of 0.01 m were used in the initial crack generation in the numerical model. Fig. 14 shows the nominal strength versus the specimen size, that clearly demonstrates the size effect. By adjusting the α parameter, a size effect curve similar to that of a given rock can be obtained.

5. CONCLUSION

The capability of a discrete element numerical model in simulating size effect in rock was examined in this paper. It was shown that:

- Numerical specimens without initial cracks did not show size effect with the same intensity as observed for many rocks.
- Beams and tensile specimens with a single initial notch or crack showed size effect consistent with that expected from linear fracture mechanics.
- A compressive numerical specimen with an initial crack length proportional to specimen size and oriented to induced mixed mode failure, could not simulate extensive size effect.
- Compressive specimens with initial random cracks could simulate size effect if the average crack length increases as an exponential function of specimen size.

The numerical model, if considered as a fair representation of rock behavior, indicates that size effect in rock is due to presence of fissures in rock. Although fracture mechanics can explain size effect in tensile and bending tests, for compression tests, an additional factor must be involved. That was the reason that the initial cracks or flaws length were assumed to increase faster than the specimen size. This is consistent with the idea that larger specimens have greater chance of containing major initial fractures.

REFERENCES

1. Mogi, K. 1962. The influence of the dimensions of specimens on the fracture strength of rocks. *Bulletin of the earthquake research institute*. 40: 175-185.
2. Bieniawski, Z.T. 1967. The effect of specimen size on compressive strength of coal. *Int. J. Rock Mech. Min. Sci.* 5: 325-335.
3. Pratt, H. R., A.D. Black, W.S. Brown, and W.F. Brace. 1971. The effect of specimen size on the mechanical properties of unjointed diorite. *Int. J. Rock Mech. Min. Sci.* 9: 513-529.
4. Van Vliet, M.R.A. and J.G.M. Van Mier. 2000. Experimental investigation on size effect in concrete and sandstone under uniaxial tension. *Engineering fracture mechanics*. 65: 165-188.
5. Bazant Z.P. and Planas J. 1998. *Fracture and size effect in concrete and other quasibrittle materials*. CRC Press.
6. Weibull W. 1939. A statistical theory of the strength of materials. *Proceedings Royal Swedish Academy of Eng. Sci.*, 151: 1-45.
7. Griffith A.A. 1924. Theory of rupture. *Proceedings of first international congress of applied mech.*, Delft, 55-63.
8. Fakhimi A. 1998. *Theory and user manual of CA2 computer program*. Report no. 262. Building and Housing Research Center, Tehran, Iran.
9. Fakhimi, A. 2004. Application of slightly overlapped circular particles assembly in numerical simulation of rocks with high friction angles. *Engineering Geology*, 74: 129-138.
10. Fakhimi, A. and T. Villegas. 2004. Calibration of a discrete element model for rock failure envelope and tensile strength. Numerical modeling in micromechanics via particle methods, *Proceedings of the 2nd International PFC Symposium, Japan*, 383-390. eds. Shimizu, Hart and Cundall.
11. Zietlow, W.K. and J.F. Labuz. 1998. Measurement of the intrinsic process zone in rock using acoustic emission. *International Journal of Rock Mechanics and Mineral Science*. 35(3): 291-299.